HAL open science

Deep Two-phase, Hemispherical Magma Oceans on Lava Planets

Charles-Édouard Boukaré, Nicolas B. Cowan, James Badro

▶ **To cite this version:**

Charles-Édouard Boukaré, Nicolas B. Cowan, James Badro. Deep Two-phase, Hemispherical Magma Oceans on Lava Planets. The Astrophysical Journal, 2022, 936, 10.3847/1538-4357/ac8792 . insu-03824259

HAL Id: insu-03824259

https://insu.hal.science/insu-03824259v1

Submitted on 21 Oct 2022

HAL is a multi-disciplinary open access archive for the deposit and dissemination of scientific research documents, whether they are published or not. The documents may come from teaching and research institutions in France or abroad, or from public or private research centers.

L'archive ouverte pluridisciplinaire **HAL**, est destinée au dépôt et à la diffusion de documents scientifiques de niveau recherche, publiés ou non, émanant des établissements d'enseignement et de recherche français ou étrangers, des laboratoires publics ou privés.

Distributed under a Creative Commons Attribution 4.0 International License

The Astrophysical Journal, 936:148 (9pp), 2022 September 10 https://doi.org/10.3847/1538-4357/ac8792
© 2022. The Author(s). Published by the American Astronomical Society.
OPEN ACCESS

Deep Two-phase, Hemispherical Magma Oceans on Lava Planets

Charles-Édouard Boukaré[1], Nicolas B. Cowan[2,3], and James Badro[1]
[1] Institut de Physique du Globe de Paris, 1, rue Jussieu, Paris CEDEX 05, 75238, France
[2] Department of Earth and Planetary Sciences, McGill University, 3450, rue University, Montréal, Québec, H3A 0E8, Canada
[3] Department of Physics, McGill University, 3600, rue University, Montréal, Québec, H3A 2T8, Canada
Received 2022 January 25; revised 2022 August 2; accepted 2022 August 6; published 2022 September 9

Abstract

Astronomers have discovered a handful of exoplanets with rocky bulk compositions but orbiting that orbit so close to their host star that the surface of the planet must be at least partially molten. It is expected that the dayside of such "lava planets" harbors a rock-vapor atmosphere that flows quickly toward the airless nightside—this partial atmosphere is critical to the interpretation of lava planet observations, but transports negligible heat toward the nightside. As a result, the surface temperature of the magma ocean may range from 3000 K near the substellar point down to 1500 K near the day–night terminator. We use simple models incorporating the thermodynamics and geochemistry of partial melt to predict the physical and chemical properties of the magma ocean as a function of the distance from the substellar point. Our principal findings are that: (1) the dayside magma ocean is much deeper than previously thought, probably extending down to the core–mantle boundary below the substellar point of an Earth-sized planet; (2) much of the dayside is only partially molten, leading to gradients in the surface chemistry of the magma ocean; and (3) the temperature at the base of the silicate mantle is as important as the surface temperature. In the most extreme cases, lava planet interiors could be cold enough such that thermal stratification below the substellar point is gravitationally stable. These findings have important implications for the dynamics of the magma ocean, as well as the composition and dynamics of the atmosphere.

Unified Astronomy Thesaurus concepts: Exoplanet dynamics (490); Exoplanet atmospheres (487); Exoplanets (498); Extrasolar rocky planets (511)

1. Introduction

Astronomers have recently discovered a new class of planets with bulk densities suggestive of terrestrial composition, but orbiting so close to their host stars that the dayside equilibrium temperature exceeds the solidus temperature of silicates, and hence must be molten. Notable examples include CoRoT-7b (Léger et al. 2009), Kepler-10b (Batalha et al. 2011), 55 Cnc e (Demory et al. 2011; Winn et al. 2011), and K2-141b (Barragán et al. 2018; Malavolta et al. 2018). These "lava planets" are predicted to have a permanent magma ocean with an overlying rock-vapor atmosphere (Schaefer & Fegley 2009). As with most short-period exoplanets, lava planets are expected to be tidally locked into synchronous rotation (Léger et al. 2011). For a review of lava planets, see Chao et al. (2021).

1.1. Atmospheres of Lava Planets

In the likely event that a lava planet has already lost its volatiles to space, it cannot maintain a steady-state atmosphere on its nightside (Léger et al. 2011). Instead, it will have a partial atmosphere of rock vapor on the dayside that blows toward the airless nightside, cools and condenses onto the surface, only to then be returned to the substellar point via magma ocean currents and solid-state flows near the shores of the ocean (Castan & Menou 2011; Kite et al. 2016; Nguyen et al. 2020). If a lava planet somehow retains volatiles over gigayears, then it may have a global atmosphere and relatively homogenized surface temperatures (Hammond & Pierrehumbert 2017). In the current paper, we adopt the majority view, namely that lava planets have a day-to-night temperature contrast of more than 2000 K, with a dayside magma ocean and an airless nightside.

Fortunately, the high temperatures of lava planets make them amenable to observational studies. Transits, eclipses, and phase variations of lava planets have been observed with the CoRoT, Kepler, and Spitzer space telescopes (Léger et al. 2009; Batalha et al. 2011; Demory et al. 2016; Zieba et al. 2022), and further observations have been approved for the Hubble and James Webb space telescopes (e.g., Dang et al. 2021; Espinoza et al. 2021; Hu et al. 2021; Quinn et al. 2021). These measurements constrain the surface temperature of a lava planet as a function of longitude, the atmospheric composition, and even the atmospheric temperature structure (Nguyen et al. 2020; Zilinskas et al. 2020; Zilinskas et al. 2021; Nguyen et al. 2022). While remote sensing can only directly probe an exoplanet's atmosphere and surface, one may sometimes indirectly infer properties of its interior (Cowan 2014).

The atmospheric composition and dynamics on a lava planet depend on the composition and dynamics of its magma ocean. To first approximation, the atmosphere at some location on a lava planet is dictated by the saturation vapor pressure above the liquid surface (Castan & Menou 2011). The spatial variations in temperature—and hence vapor pressure—are the dominant source of the atmospheric dynamics in its atmosphere. With observations of their atmospheres becoming available, it is therefore timely to produce model predictions for the magma oceans on lava planets.

1.2. Interiors of Lava Planets

The magma ocean on a lava planet is governed by the same geochemistry and geophysics as the magma oceans that are

Original content from this work may be used under the terms of the Creative Commons Attribution 4.0 licence. Any further distribution of this work must maintain attribution to the author(s) and the title of the work, journal citation and DOI.

thought to have existed at the formation of rocky worlds in the solar system (Elkins-Tanton 2012), but with drastically different boundary conditions. The high dayside surface temperature is constant through time, set by the competition of stellar irradiation and thermal radiation. The interior of the planet should therefore cool more slowly than a long-period terrestrial planet. The magma ocean on a lava planet is horizontally heterogeneous, going from fully molten near the substellar point ($T \approx 3000$) to completely solid near the day–night terminator ($T \approx 1000$)—in other words, lava planets cannot be treated as spherical cows.

Previous models of lava planet interiors have assumed that the dayside magma ocean is shallow (Léger et al. 2011; Kite et al. 2016; Nguyen et al. 2020). Using a liquidus temperature gradient of about 30 K GPa^{-1} (Solomatov 2000), previous authors have predicted that the temperature of the magma pond intersects the planet's liquidus temperature at a depth of about 70 km.

However, for a multicomponent system, such as the bulk silicate Earth (BSE), the liquidus does not characterize the temperature at which magma becomes solid. The magmas composed of several oxides, such as MgO, FeO, SiO_2, or CaO, fully solidify only when the temperature drops below the solidus. For temperatures between the solidus and the liquidus, the magma is partially molten. There is a rheological transition at about 50% of the melt fraction, where the magma starts to behave as a solid rather than a liquid (e.g., Abe 1993; Lejeune & Richet 1995; Costa 2005). We show here that even though the temperature in the magma pond intersects the liquidus at a shallow depth, the temperature in the deeper part of the planet remains close the liquidus, due to latent heat effects.

Major advances in the laser-heated diamond anvil cell (LHDAC) technique now give direct access to pressures and temperatures relevant to the deep interior of terrestrial planets. Recent measurements of liquidus and solidus temperatures via LHDAC (e.g., Fiquet et al. 2010; Andrault et al. 2011, 2012, 2014; Tateno et al. 2014; Pradhan et al. 2015; Tateno et al. 2018) show that the temperature difference between liquidus and solidus for Earth-like material can be as small as 400 K (Andrault et al. 2011) and as large 1000 K (Fiquet et al. 2010). Using these recent experimental data at high pressures, we show that hemispherical magma oceans in lava planets are most likely deep and probably extend down to the core–mantle boundary (CMB) for surface temperatures as low as 1900 K.

In Section 2, we present our assumptions and describe how we compute the interior temperature profile of a lava planet. In Section 3, we present our results regarding the magma ocean depth, the location of the shore, and the potential chemical gradients within the magma ocean due to partial crystallization. In Section 4, we speculate about the global internal dynamics of lava planets, its effect on atmospheric composition, and future spectroscopic observations.

2. Model

We consider a tidally locked planet of about 1.5 Earth radii that orbits close to its parent star. Since the overlying atmosphere is optically thin, the planet's surface temperature is well approximated by local radiative equilibrium (Léger et al. 2009; Castan & Menou 2011; Nguyen et al. 2020). The large angular size of the star, as seen from the planet, leads to an extended penumbra region and less than a hemisphere in the dark (Léger et al. 2011; Nguyen et al. 2020); and we adopt a temperature at the substellar point appropriate for K2-141b, $T_{ss} = 3000$ K. As we shall see, our model can easily be applied to cooler lava planets. We also assume that the composition of the lava planet is that of BSE (Palme & O'Neill 2003).

On the dayside, lava planets are expected to be fully molten for surface temperatures greater than 1700 K, forming a magma ocean (e.g., Kite et al. 2016). As the temperature decreases toward the nightside, the melt fraction at the surface of the planet should also decrease. The location of the shore is determined by (1) the variation of the surface temperature with respect to the angular distance from the substellar point, and (2) the melting temperature of silicates at low pressure. Similarly, the depth of the magma ocean is constrained by (1) the interior temperature profile, and (2) the melting temperature of silicates at high pressures.

The interior thermal structure of the planet has a first-order control on the planet's dynamics, as it governs the relative size of the magma ocean compared to the solid mantle. Both the depth and lateral extent of the magma ocean have a primary role in the atmosphere–interior coupling. Indeed, the rates of heat and mass transfer differ by several orders of magnitude between solid and liquid states. For tidally locked lava planets, the temperature difference between the two hemispheres is expected to drive horizontal convection (e.g., Hughes & Griffiths 2008). In this regime, heat transport proceeds horizontally, similar to the thermohaline circulation in the Earth's oceans. The high surface temperature of a lava planet does not necessarily preclude the possibility of Rayleigh–Bénard-like convection. Indeed, the base of the rocky mantle is likely hotter than the surface, due to the slowly cooling iron core. In this study, we distinguish two endmember scenarios depending on the temperature difference between the surface and the base of the silicate mantle; that is, the CMB.

We define the hot-core scenario as cases where the temperature between the surface and the CMB is large enough to drive vertical thermal convection, imposing an adiabatic temperature gradient in the mantle. The necessary condition for vertical, i.e., Rayleigh–Bénard-like, thermal convection is that the temperature difference between the surface and the CMB is superadiabatic, i.e., the Schwarzschild criterion. We define the cold-core scenario as cases where the temperature difference between the surface and the CMB is subadiabatic. We use the present-day Earth's CMB temperature as the lowest possible Earth-sized lava planet's CMB temperature. The modern Earth has a surface temperature of about 300 K and the CMB temperature is about 4000 K (e.g., Hernlund et al. 2005; Fiquet et al. 2010; Andrault et al. 2011). For a planet with a higher radiative equilibrium surface temperature—including lava planets—the CMB temperature is likely to be higher than the Earth's at the same age. By the same token, super-Earths likely have greater internal temperatures, due to their greater mass-to-surface area ratio. Hence, the CMB temperature on a lava planet is expected to be at least as high as the surface temperature at the substellar point, generating a flow of heat from the interior to the surface, and possibly driving convective motions.

In this study, we aim to estimate a pseudo-steady-state interior thermal structure of lava planets. The heart of this work is the computation of adiabatic profiles at pressure and temperature conditions relevant for a lava planet's interior. In the context of short-orbit planets with high surface temperatures, interior

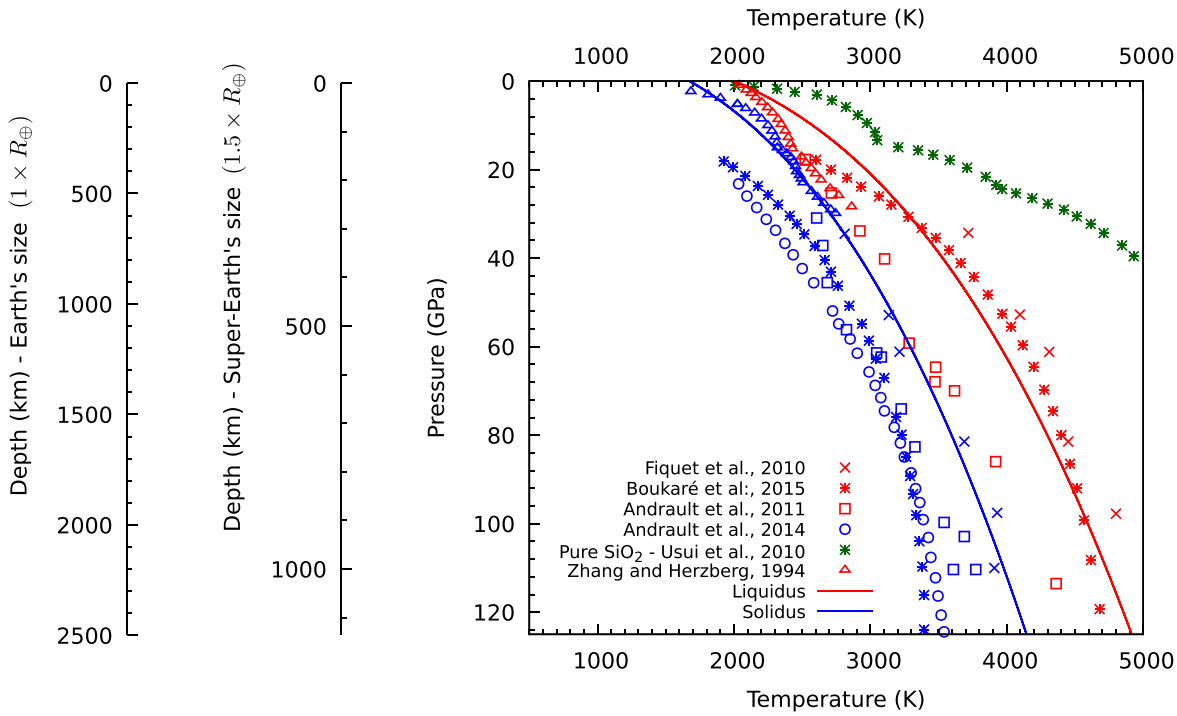

Figure 1. High-pressure liquidus (red) and solidus (blue) temperatures for Earth-like mantle compositions. Above the liquidus temperature, silicates are liquid. When the temperature lies between the liquidus and the solidus, silicates are partially molten. Silicates fully solidify when the temperature drops below the solidus. The colored symbols show recent experimental measurements (Zhang & Herzberg 1994; Fiquet et al. 2010; Andrault et al. 2011, 2014) and theoretical calculations (Usui & Tsuchiya 2010; Boukaré et al. 2015) of the liquidus and solidus temperatures at high pressures. Discrepancies among the data in the literature arise from the differences in approaches, such as the silicate compositions or melt detection techniques. For the sake of simplicity, we approximate the liquidus and solidus curves for Earth-like composition using the red and blue lines, Equations (1) and (2). On the left, pressure–depth conversions are shown for the Earth and a $1.5R_\oplus$ super-Earth. Note that the melting curve of pure SiO_2, shown by the green asterisks, substantially overestimates the liquidus temperature of the BSE.

adiabats are fundamentals, as they control whether the temperature difference between the surface and the interior is sufficient to drive vertical heat transport by convection. We then compare the interior temperature profiles with melting curves of silicates to determine whether silicates are solid or liquid. We neglect multiphase mechanical processes, such as crystal settling, solidification dynamics, and melt percolation on the planet's structure (e.g., Maas & Hansen 2015; Boukaré & Ricard 2017).

2.1. Liquidus and Solidus Temperatures

Two temperatures are required to describe the melting behaviors of silicate materials. Above the liquidus temperature, silicates are fully liquid. Below the solidus temperature, silicates are fully solid. Silicates are partially molten for temperatures that lie between the solidus and the liquidus. This is different from "pure species," such as SiO_2 or MgO, whose phase change occurs at a single temperature. Both liquidus and solidus temperature are functions of pressure and composition.

High-pressure liquidus and solidus temperatures of the BSE are an area of active research (Fiquet et al. 2010; Andrault et al. 2011, 2012, 2014). To propose a conservative estimate of the hemispherical magma ocean depth, we use the experimental data of Fiquet et al. (2010)—the highest reported liquidus temperature. Our model thus provides a lower bound on the magma ocean depth. The experimental data of Andrault et al. (2011), for example, suggest a lower liquidus temperature, and hence favor a deeper magma ocean.

The solidus and liquidus temperatures are fitted to the experimental data of Fiquet et al. (2010) and Zhang & Herzberg (1994). The liquidus, T_l, and solidus, T_s, are plotted in Figure 1 and given by

$$T_l(P) = 2000\ \mathrm{K}\left(0.1169\left(\frac{P}{\mathrm{GPa}}\right) + 1\right)^{0.32726}, \tag{1}$$

$$T_s(P) = 1674\ \mathrm{K}\left(0.0971\left(\frac{P}{\mathrm{GPa}}\right) + 1\right)^{0.351755}. \tag{2}$$

2.2. Isentropic Temperature Profiles

The temperature profile in the fully molten region is calculated using the isentropic (and thus adiabatic) temperature gradient of a one-phase system,

$$\left(\frac{\partial T}{\partial P}\right)_S^{\mathrm{op}} = \frac{\alpha V}{C_p} T, \tag{3}$$

where α is the thermal expansion, V is the volume, and C_p is the thermal capacity of the silicate melt. A self-consistent integration of Equation (3) requires a thermal equation of state (EoS) for silicate melt. We use

$$P(V, T) = 3K_0 f^{-2}(1 - f)e^{\frac{3}{2}(K'-1)(1-f)} + \alpha_0 K_0 f^{3q-3}(T - T_0), \tag{4}$$

where the dimensionless length is $f = (V/V_0)^{1/3}$, K_0 and α_0 are the isothermal bulk modulus and thermal expansion at the reference conditions (V_0 and T_0), and $K' = (\partial K_0/\partial P)_V$ and q are constants. The first term on the right-hand side of Equation (4) corresponds to the Vinet–Rydeberg isothermal

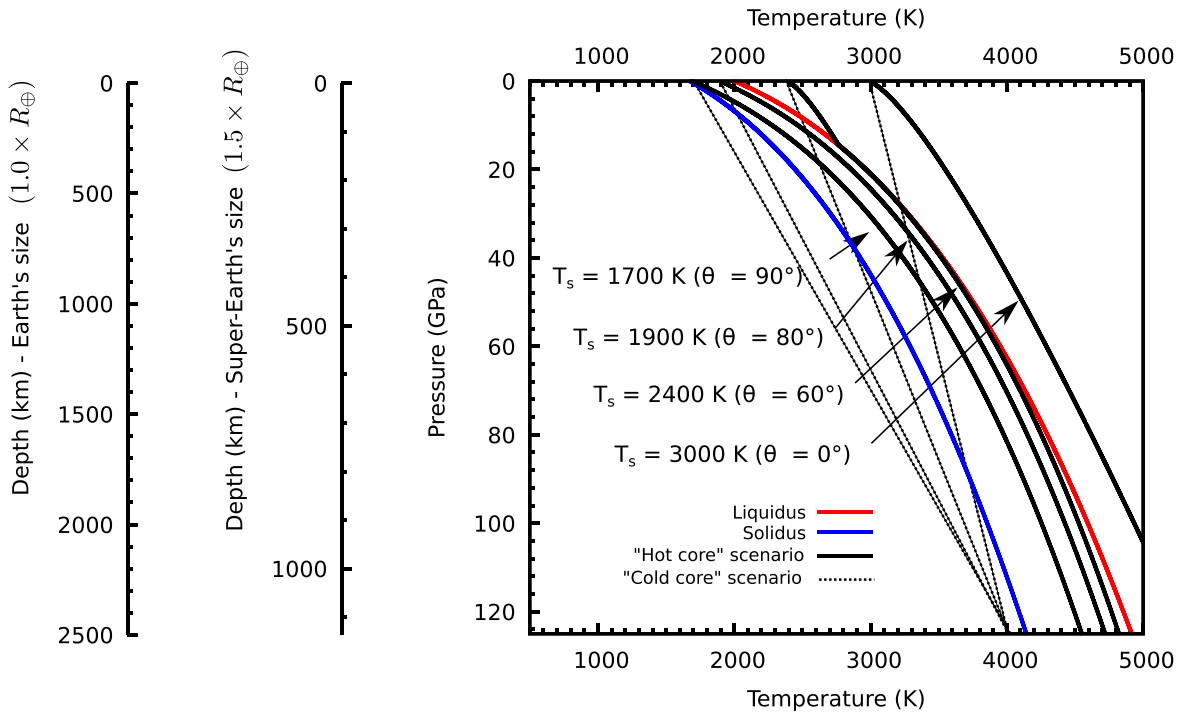

Figure 2. Adiabatic and subadiabatic temperature profiles of lava planet interiors for four different surface temperatures: 1700, 1900, 2400, and 3000 K. We consider two endmember scenarios, depending on the iron core temperature. In the hot-core scenario, the temperature difference between the surface and the CMB is large enough to drive thermal convection, imposing an adiabatic temperature profile (solid black lines) in the magma ocean. In the cold-core scenario, the temperature difference between the surface and the CMB is subadiabatic, preventing heat transport by convection. We use the present-day Earth's CMB temperature, i.e., 4000 K, as a lower bound for an Earth-sized lava planet's CMB temperature in the cold-core case. For the hot-core scenario, the temperature increase with depth is due to the isentropic compression of the material. In regions hotter than the liquidus, the temperature follows a one-phase homogeneous isentrope (or adiabat). When the temperature is between the liquidus and the solidus, entropy conservation must account for the latent heat of fusion. In this region, the temperature follows a two-phase isentrope, akin to moist adiabats of planetary atmospheres. For a surface temperature of 3000 K in a hot-core scenario, the silicate mantle is expected to be fully molten for a planet the size of Earth or a $1.5R_\oplus$ super-Earth. For the same surface temperature, the magma ocean is still expected to be 1000 km deep below the substellar point for an Earth-sized lava planet, even if the CMB temperature is as low as 4000 K. For a surface temperature of 2400 K, the adiabat intersects the liquidus at a depth of about 100 km for a $1.5R_\oplus$ super-Earth. However, the adiabat remains very close to the liquidus at greater depth, such that the interior is still expected to be mostly molten in a hot-core case (see Figure 3).

EoS (Vinet et al. 1987), while the second term is the thermal pressure as initially proposed for solids (Anderson 1979). Whereas the description of the thermal pressure for solids requires positive values of q, liquids are generally described by negative values of q (Asimow & Ahrens 2010; Boukaré et al. 2015). We fitted the thermodynamic data of Boukaré et al. (2015) with Equation (4). We use $V_0 = 26.27$ cm^3 mol^{-1}, $T_0 = 298$ K, $\alpha_0 = 10.8 \times 10^{-5}$ K^{-1}, $K_0 = 17.58$ GPa, $K' = 6.9$, and $q = -3.37$.

In the partially molten region, the temperature profile follows a two-phase adiabat (e.g., Miller et al. 1991; Asimow & Ghiorso 1998) akin to moist adiabats in planetary atmospheres,

$$\left(\frac{\partial T}{\partial P}\right)_S^{\mathrm{tp}} = \frac{\left(\frac{\partial T}{\partial P}\right)_S^{\mathrm{op}} - \frac{T\Delta S}{C_p}\left(\frac{\partial F}{\partial T}\right)_P\left(\frac{\partial T_m}{\partial P}\right)_F}{1 - \frac{T\Delta S}{C_p}\left(\frac{\partial F}{\partial T}\right)_P}, \tag{5}$$

where ΔS is the entropy difference between the liquid and the solid phase, F is the melt fraction, $(\partial F/\partial T)_P$ is the variation of the melt fraction with temperature at constant pressure, and $(\partial T_m/\partial P)_F$ is the variation of the equilibrium temperature with pressure at constant melt fraction. Rigorous application of Equation (5) requires detailed self-consistent phase diagrams to constrain the latter parameters. The latent heat goes as $T\Delta S \propto TR$ and the thermal capacity as $C_p \propto 3R$, so we assume that $T\Delta S/C_p \propto T$, following Miller et al. (1991). To validate this assumption, we ran calculations using the thermodynamic model of Boukaré et al. (2015), confirming that $\Delta S/C_p$ is of the order of unity. We use the crude assumption that the melt fraction varies linearly between the liquidus and the solidus at fixed pressure, so that

$$\left(\frac{\partial F}{\partial T}\right)_P = \frac{1}{T_l(P) - T_s(P)}, \tag{6}$$

where $T_l(P)$ and $T_s(P)$ are the liquidus and solidus temperatures at pressure P, respectively.

3. Results

3.1. Magma Ocean Depth

Our calculations show that the magma ocean on the permanent dayside of a lava planet is deeper than previously thought (see Figure 2) for both the hot-core and cold-core scenarios. For a surface temperature of 3000 K in the hot-core scenario, the interior temperature remains above the liquidus temperature at least up to 130 GPa, i.e., 1200 km in a $1.5R_\oplus$ super-Earth. For a surface temperature of 2400 K, the interior temperature intersects the liquidus at about 15 GPa, i.e., 150 km in a $1.5R_\oplus$ super-Earth, but it remains close to the liquidus at higher pressures. This is due to latent heat effects that bend adiabats, such that they remain approximately parallel to the liquidus. The latter is controlled by the second term on

the numerator of the right-hand side of Equation (5). For a surface temperature of 1700 K, the interior temperature is halfway between the liquidus and the solidus temperature from the surface down to 120 GPa. These results are in excellent agreement with previous models of Earth's magma ocean (e.g., Abe 1997; Solomatov 2000; Thomas et al. 2012; Lebrun et al. 2013; Monteux et al. 2016).

For the cold-core scenario, the subadiabatic thermal stratification follows a conductive profile that connects the surface temperature to the CMB temperature (see Figure 3). For the sake of simplicity, we neglect for now horizontal thermal convection as well as compositional convection. We assume that a fluid column that is thermally stable with regard to gravity is motionless. Latent heat and compression effects are suppressed as the magma is static, the fluid being stably stratified. This assumption thus provides a conservative estimate of the magma ocean depth in the cold-core scenario. A self-consistent fluid dynamics description is required to go beyond this first-order assumption. For a surface temperature of 3000 K, this temperature stratification implies a 1000 km deep magma ocean on a $1R_{\oplus}$ lava planet, and a 500 km magma ocean on a $1.5R_{\oplus}$ lava planet. For a surface temperature of 1900 K, the magma ocean is expected to be only 100 km deep on a $1.5R_{\oplus}$ lava planet. The magma ocean depth rapidly drops as the surface temperature decreases in the cold-core scenario. This is because the thermal profiles are not affected by the melting curves when the silicates are immobile. Our calculations show that stellar irradiation can generate a thermally stable stratification in the magma ocean and inhibit thermal convection below the substellar point for CMB temperatures as low as 4000 K. As the CMB temperature of a lava planet is difficult to constrain a priori, we envision in the discussion section different scenarios, depending on whether the temperature difference between the surface and the interior is superadiabatic or subadiabatic.

We use Equation (6) to determine the melt fraction as a function of depth for different surface temperatures, shown in Figure 3. Our calculations indicate that the melt fraction in the magma ocean stays above 50% for surface temperatures hotter than 1700 K. As the rheological transition between solid and liquid occurs at about 50% of the melt fraction, these results show that the hemispherical magma ocean behaves as a liquid for surface temperatures as low as 1700 K. For a melt fraction close to the rheological transition, the multiphase mixture is expected to flow as a sluggish fluid—not as a solid.

Our temperature and melt fraction profiles (Figures 2 and 3) can be used as first-order estimations of the interior structures of lava planets in two cases. Our findings apply either to (1) multiple lava planets with different surface temperatures at the substellar point, or (2) different locations in the same lava planet. If we neglect thermal mixing in the deep interior, these profiles can be used as a crude proxy for evaluating the effects on the interior thermal structure of lateral temperature variations imposed at the surface. Adopting this strong assumption for K2-141b, the interior profiles for surface temperatures of 1700, 2000, 2400, and 3000 K correspond to angular distances from the substellar point of $\theta = 90°$, $\theta = 80°$, $\theta = 60°$, and $\theta = 0°$.

3.2. Where is the Magma Ocean Shore?

Temperature decreases away from the substellar point. Eventually, the temperature drops below the liquidus. We use the software MELTS 1.2.0 to compute the crystallization sequence of magma with a BSE composition at shallow depth, i.e., 250 bar. For the sake of simplicity, we only consider the case of batch crystallization where the crystals remain in chemical equilibrium with the melt during solidification. These thermodynamic calculations allow us to predict more precisely the evolution of the melt composition in major and minor elements, as well as the liquidus and solidus temperatures at the surface of the planet. These temperatures constrain the location of the shore.

For Kepler K2-141b, with a substellar surface temperature of 3000 K, the transition from fully liquid to partially molten occurs near $\theta = 80°$. The solidus temperature is reached at $\theta = 100°$. There is no well-defined shores at the surfaces of lava planets, but rather a gradual transition from the molten to the solid hemisphere. It must be noted that the partially molten region will be larger for lava planets with more modest substellar temperatures. For example, K2-22b has a substellar surface temperature of 2000 K, resulting in a partially molten region that extends from $\theta = 0°$ to $\theta = 80°$.

3.3. Chemical Fractionation in the Magma Ocean

Our calculations of the magma crystallization sequence (Figure 4) offer the possibility of predicting the compositional variation induced by solidification at the surface of a lava planet. Upon solidification, incompatible species stay in the melt, instead of precipitating as minerals. Incompatible species, such as Na_2O, K_2O, or H_2O, are thus concentrated in the melt as crystallization proceeds (see Figure 4). Since the melt fraction is primarily controlled by temperature, we propose that the lateral variation of surface temperature generates compositional heterogeneities in lava planets by incongruent melt solidification.

Moreover, our modeling indicates that an additional fluid phase composed mostly of H_2O exsolves from the melt as the temperature approaches the solidus. Here, H_2O will degas, because its concentration in the melt has increased to the point of saturation. This can be seen in Figure 4, in the plateau of the magma water content close to the solidus temperature. This process is different from atmosphere formation by liquid-vapor equilibrium at the planet's surface. At the liquid–gas interface, pressure is set by vapor exsolution itself. In the planet interior, pressure is set by the geostatic pressure. In that case, H_2O degassing is more akin to the behavior of salt in water. When water is saturated in salt, any increase in salt content results in salt exsolution.

4. Discussion

4.1. Implications for Lava Planet Interior Structures and Dynamics

In this work, we consider two extreme cases for the temperature profile of the silicate mantle: adiabatic and subadibatic. The reality is most likely a complex combination of these two endmembers that cannot be captured in 1D studies. For instance, it would not be surprising if the thermal profile is subadiabatic below the substellar point—where the temperature difference between the surface and the interior is the smallest, and becomes progressively adiabatic near the terminator.

Based on these thermodynamics calculations, we propose a new model for the interior structure of lava planets (Figure 5). On the dayside, the magma ocean is at least 500 km deep and

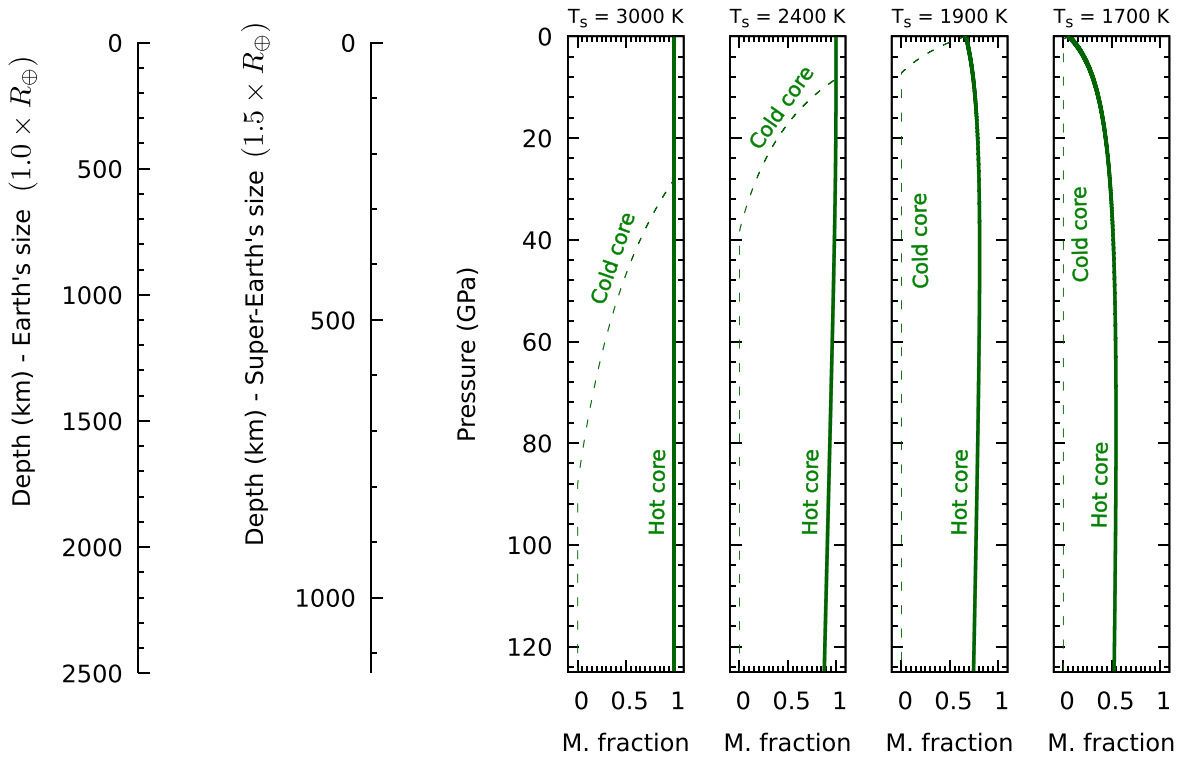

Figure 3. The melt fraction as a function of depth for four surface temperatures: 3000, 2400, 1900, and 1700 K. The rheological transition between solid-like and liquid-like behavior occurs at about a 50% melt fraction. For the hot-core case (see the main text), the bulk of the magma ocean therefore behaves as a sluggish fluid—not a solid—for surface temperatures as low as 1700 K. For the cold-core scenario (see the main text), the magma behaves as a liquid down to 50 GPa for a substellar temperature of 3000 K, but only a shallow magma ocean of about 100 km remains for a surface temperature of 1900 K.

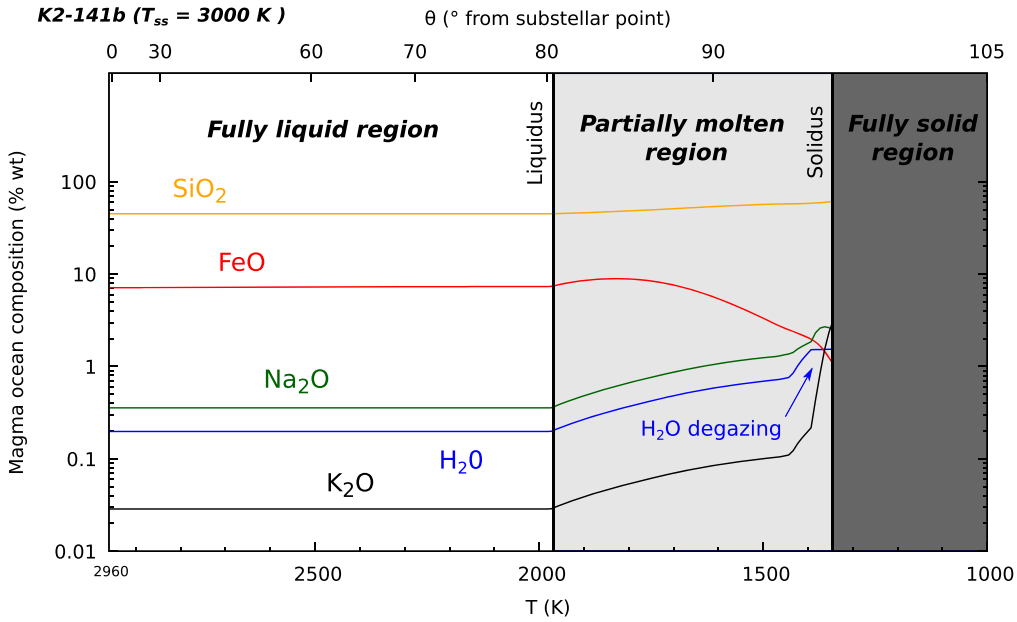

Figure 4. Lateral variation of the surface composition of tidally locked lava planets. Concentrations of SiO_2 (yellow), FeO (red), Na_2O (green), H_20 (blue), and K_2O (black) as a function of surface temperature (bottom axis) or distance from the substellar point on K2-141b (top axis). There is no well-defined magma ocean shore, but rather a gradual transition from the molten to the solid hemisphere. In this partially molten region, the composition of the magma changes, as precipitating minerals do not have the same composition as the melt. Depending on the style of convective dynamics, these chemical heterogeneities can be mixed back into the convective region or permanently hidden from the surface. For instance, enrichment in FeO would promote the formation of very dense melt that might sink to the bottom of the magma ocean (Kite et al. 2016). Additionally, the concentration of volatile species, such as H_2O and CO_2, can eventually reach the saturation limit in the melt near the solidus. When the melt is saturated, any increase in concentration results in the formation of bubbles that degas at the surface of the planet, with possible implications for transit observations of lava planets.

most likely extends down to the CMB, if the hot-core scenario is favored. One must also recall that our cold-core scenario gives a very conservative estimate of the magma ocean depth, as super-Earth lava planets are expected to have a higher interior temperature than the Earth at the same age. Temperature gradients at the surface probably drive shallow horizontal

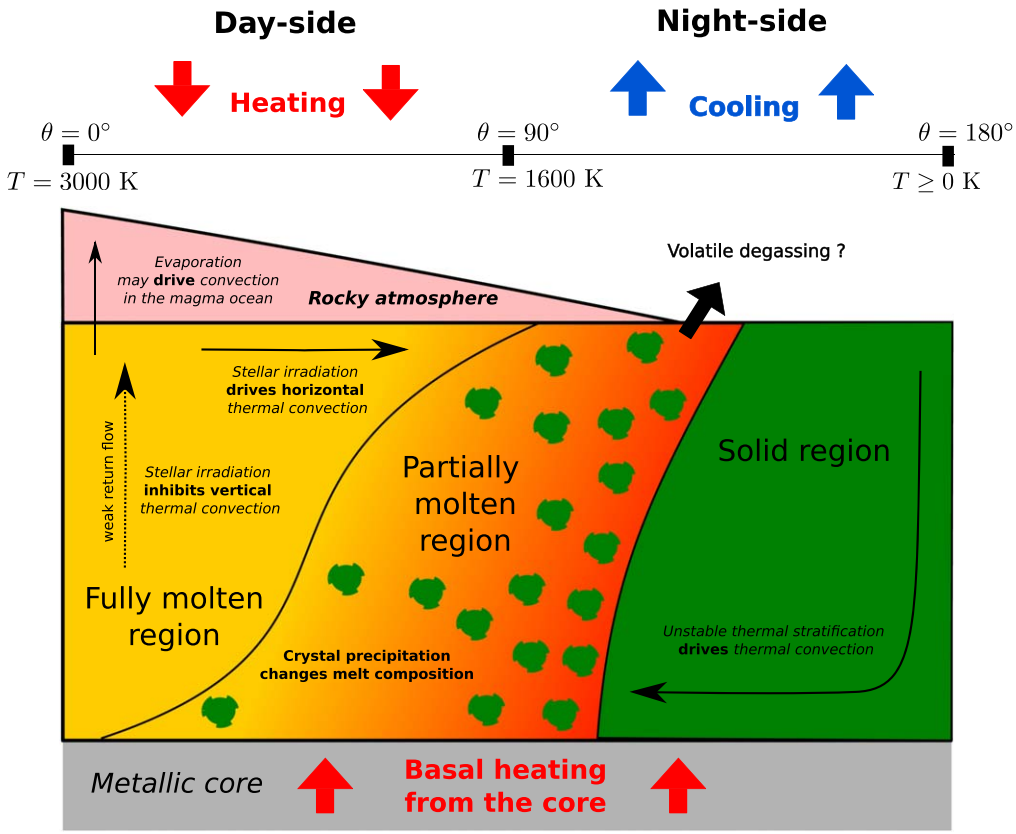

Figure 5. Schematic of the interior structure and dynamics of a lava planet in the hot-core scenario (see the main text). The hemispherical magma ocean on the dayside could extend down to the CMB. The nightside mantle is solid. A partially molten region probably connects the two hemispheres. The illustrated pseudo-steady-state structure involves fluid motions. The solid–liquid interfaces are not static, rather rocky materials are expected to flow through the solid–liquid interface, melting or solidifying at these boundaries, depending on the flow direction. The surface temperature gradient drives the magma currents between the dayside and the nightside. Temperature differences between the CMB and the planetary surface are expected to drive convection of the rocky mantle. Geodynamic models are required to explore the horizontal convective dynamics, as well as the efficiency of the solid–liquid phase separation and chemical mixing.

convection from the dayside to the nightside. The crystal fraction increases progressively toward the nightside, enriching the melt in incompatible elements. This process may be able to progressively differentiate the magma ocean, depending on the efficiency of the phase separation and the chemical mixing in the interior. Compositional and density differences between the melt and solids might have complex feedback with the interior fluid dynamics of lava planets. For instance, liquid silicates might become denser than their solid counterparts at high pressures (Funamori & Sato 2010; Boukaré et al. 2015; Boukaré & Ricard 2017; Caracas et al. 2019). On the nightside, the temperature stratification is expected to be superadiabatic, driving thermal downwellings. It is difficult to predict whether these downwellings occur in the solid or partially molten region. The return flow below on the dayside is probably slow, as the thermal stratification may be gravitationally stable below the substellar point. Only a high core temperature can sustain an adiabatic temperature stratification below the substellar point. For an Earth-sized lava planet with a surface temperature of 3000 K, the CMB temperature must be hotter than 5500 K. Compared to previous studies that suggest a shallow magma ocean, our modeling points toward a deep hemispherical magma ocean, with profound implications for the atmosphere. Indeed, the composition of the atmosphere is dictated by the replenishment of surface material with fertile material coming from the magma ocean.

Our work also raises the importance of the CMB temperature for the interior dynamics of lava planets. An interesting outcome is that the hot-core and cold-core scenarios would produce very different magma ocean dynamics, with very different implications for the overlying atmosphere. In the hot-core scenario, lava planets are expected to have a deep and large magma ocean that convects vigorously, quickly providing fresh material to the atmosphere. In the cold-core scenario, magma oceans on lava planets might instead be a stagnant fluid layer. For instance, if one could deduce from the composition of the atmosphere whether the underlying magma ocean convects or not, our adiabats could be used to quantitatively constrain the temperature of the planet's deep interior.

The CMB temperature of a lava planet might tell a lot about its history. If the planet cooled for gigyears before migrating to its current small semimajor axis, its CMB temperature is most likely cold. In that case, its long-term thermal history might have followed that of the Earth. On the other hand, if the planet migrated while still young—or formed "in situ"—very close to its parent star, the interior might have experienced a slower cooling that the Earth. Such lava planets might have a high CMB temperature that would allow vigorous convection even below the substellar point. It is important to mention that the hot-core scenario may not be a viable long-term dynamic state. Indeed, efficient cooling by convection in the liquid state is actually expected to cool the iron core quite rapidly. This may then be used to constrain the age of the planet.

Our calculations can be considered as a first-order estimation that must be complemented by geodynamic models. Future high-pressure studies are also required to constrain liquidus

temperatures at conditions relevant for the deep mantles of super-Earths, up to about 400 GPa for a $1.5R_{\oplus}$ super-Earth with a core–mantle ratio similar to that of the Earth. However, this study raises interesting questions regarding the interior dynamics of lava planets. Fractionation by liquid–gas equilibrium at the surface has been proposed in several studies (e.g., Schaefer & Fegley 2009; Kite et al. 2016). Here, we emphasize the role of solid–liquid fractionation in the planet's interior. How do convective dynamics transition from the molten region to the solid hemisphere? How do the compositional differences between the melt and solid affect the interior dynamics? How does magma ocean composition evolve with time? How do mixing and fractionation compete to determine the steady-state composition of the magma ocean? Since the atmosphere forms in equilibrium with the magma, any processes that control its composition at the surface are crucial for the atmosphere. Therefore, magma ocean interior dynamics must be considered as a fundamental aspect of the atmospheric evolution of lava planets.

4.2. Implications for (Incompatible) Volatile Elements

Models of magma oceans generally consider the liquid–gas equilibrium at the planet surface as a primary mechanism for atmosphere formation (e.g., Abe & Matsui 1986; Bower et al. 2022). However, vapor can also degas from the melt at depths when it becomes supersaturated in volatile, as observed in terrestrial volcanoes (e.g., Le Guern et al. 1979; Tazieff 1994). This process might be an alternative to surface degassing when the magma ocean is isolated from the atmosphere by a solid conductive lid (e.g., Bower et al. 2022), and thus reinforces the efficiency of a lava planet in degassing its volatile content in regions where the surface temperature is below the solidus, i.e., near the terminator and on the nightside.

In the context of a rocky atmosphere, the fate of this putative volatile atmosphere is uncertain, however. We expect strong winds from the dayside to the nightside. Studies of lava planet atmospheres have focused on Na, because of its relative volatility (Castan & Menou 2011; Kite et al. 2016; Nguyen et al. 2020), or SiO, because of its abundance in the mantle (Nguyen et al. 2020, 2022; Zieba et al. 2022). In either case, the atmosphere is expected to flow toward the day–night terminator at velocities of kilometers per second, often exceeding the speed of sound. It has generally been assumed that any water present at the surface of the planet would be lost to space or cold trapped on the perpetually dark regions of the planet. It is possible, however, that the gradual resurfacing of the nightside due to mantle overturn could resupply water to the magma ocean. In that case, we predict that water would be degassed near the day–night terminator, only to be swept to the nightside of the planet by the background SiO wind. The presence of volatile species near the planet terminator could be tested in the near future with transit spectroscopy.

5. Conclusion

We have used state-of-the-art 1D models to make first-order predictions for the magma ocean on a lava planet. While these models are standard for solar system studies, they have not yet been widely adopted in the context of exoplanets. The keys to our results are the concept of partial melt and the high-pressure thermodynamics of melting curves.

A rocky planet's mantle is a multicomponent system, and hence it has a gradual transition from liquid to solid, rather than the sharp phase transitions of pure substances like water. As a result, a lava planet has no well-defined shore, but rather a swath thousands of kilometers wide where magma becomes increasingly sluggish.

The partial melting is also thermodynamically important: latent heat from the phase transition ensures that the isentrope is closer to isothermal, and hence the transition to solid, or even sluggish liquid, occurs at higher pressures. If the temperature difference between the surface and the iron core is large enough to drive vertical thermal convection, we predict that the magma ocean on K2-141b extends down to the CMB. For a subadiabatic temperature profile, its magma ocean is expected to be at least 500 km deep.

The interior temperature—more precisely, the CMB temperature—is as important as the surface temperature regarding the interior dynamics of lava planets. Indeed, if the temperature of the CMB is cold enough such that the temperature difference between the substellar point and the CMB is subadiabatic, magma currents below the substellar point might be very weak or even nonexistent.

Partial crystallization near the edge of the magma ocean leads to gradients in the surface composition of the melt, and hence may affect the composition of the overlying rock-vapor atmosphere. Near the mush–solid interface, the melt becomes saturated in water, resulting in the exsolution of water near the day–night terminator. Future work is needed to predict whether this could be a steady-state phenomenon or whether the water becomes permanently trapped as ice sheets on the planet's nightside.

Finally, we have adopted vertical temperature profiles in the magma ocean, but the substantial horizontal gradients in temperature, chemistry, evaporation, and precipitation likely lead to magma ocean dynamics that are completely different from those considered in the solar system context. Future challenges include numerically simulating the dynamics of lava planet magma oceans, and coupling such simulations to the atmospheric chemistry and dynamics that are probed by astronomical observations.

We thank the anonymous reviewer for the insightful comments that helped improve the paper. This work has received funding from the European Research Council (ERC) under the European Union's Horizon 2020 research and innovation program (grant agreement No. 101019965 SEPtiM). Parts of this work were supported by the UnivEarthS Labex program at Université de Paris and IPGP (ANR-10-LABX-0023 and ANR-11-IDEX-0005-02). We acknowledge the camaraderie and support of the McGill Space Institute and the "Institut de recherche sur les exoplanètes" (iREX).

ORCID iDs

Charles-Édouard Boukaré https://orcid.org/0000-0002-9265-4209
Nicolas B. Cowan https://orcid.org/0000-0001-6129-5699
James Badro https://orcid.org/0000-0001-9337-4789

References

Abe, Y. 1993, Litho, 30, 223
Abe, Y. 1997, PEPI, 100, 27
Abe, Y., & Matsui, T. 1986, JGRB, 91, E291

Anderson, O. L. 1979, JGR, 84, 3537
Andrault, D., Bolfan-Casanova, N., Nigro, G. L., et al. 2011, E&PSL, 304, 251
Andrault, D., Pesce, G., Bouhifd, M. A., et al. 2014, Sci, 344, 892
Andrault, D., Petitgirard, S., Nigro, G. L., et al. 2012, Natur, 497, 354
Asimow, P. D., & Ahrens, T. J. 2010, JGR, 115, B10209
Asimow, P. D., & Ghiorso, M. S. 1998, AmMin, 83, 1127
Barragán, O., Gandolfi, D., Dai, F., et al. 2018, A&A, 612, A95
Batalha, N. M., Borucki, W. J., Bryson, S. T., et al. 2011, ApJ, 729, 27
Boukaré, C.-E., & Ricard, Y. 2017, GGG, 18, 3385
Boukaré, C.-E., Ricard, Y., & Fiquet, G. 2015, JGRB, 120, 6085
Bower, D. J., Hakim, K., Sossi, P. A., & Sanan, P. 2022, PSJ, 3, 93
Caracas, R., Hirose, K., Nomura, R., & Ballmer, M. D. 2019, E&PSL, 516, 202
Castan, T., & Menou, K. 2011, ApJL, 743, L36
Chao, K.-H., deGraffenried, R., Lach, M., et al. 2021, ChEG, 81, 125735
Costa, A. 2005, GeoRL, 32, L22308
Cowan, N. B. 2014, EOSTr, 95, 209
Dang, L., Cowan, N. B., Hammond, M., et al. 2021, JWST Proposal Cycle, 1, #2347
Demory, B.-O., Gillon, M., de Wit, J., et al. 2016, Natur, 532, 207
Demory, B. O., Gillon, M., Deming, D., et al. 2011, A&A, 533, A114
Elkins-Tanton, L. T. 2012, AREPS, 40, 113
Espinoza, N., Bello-Arufe, A., Buchhave, L. A., et al. 2021, JWST Proposal. Cycle, 1, #2159
Fiquet, G., Auzende, A. L., Siebert, J., et al. 2010, Sci, 329, 1516
Funamori, N., & Sato, T. 2010, E&PSL, 295, 435
Hammond, M., & Pierrehumbert, R. T. 2017, ApJ, 849, 152
Hernlund, J. W., Thomas, C., & Tackley, P. J. 2005, Natur, 434, 882
Hu, R., Brandeker, A., Damiano, M., et al. 2021, JWST Proposal. Cycle, 1, #1952
Hughes, G. O., & Griffiths, R. W. 2008, AnRFM, 40, 185
Kite, E. S., Fegley, B., Jr., Schaefer, L., & Gaidos, E. 2016, ApJ, 828, 80
Le Guern, F., Carbonnelle, J., & Tazieff, H. 1979, JVGR, 6, 27
Lebrun, T., Massol, H., Chassefière, E., et al. 2013, JGRE, 118, 1155
Léger, A., Grasset, O., Fegley, B., et al. 2011, Icar, 213, 1
Léger, A., Rouan, D., Schneider, J., et al. 2009, A&A, 506, 287
Lejeune, A.-M., & Richet, P. 1995, JGRB, 100, 4215
Maas, C., & Hansen, U. 2015, JGRB, 120, 7508
Malavolta, L., Mayo, A. W., Louden, T., et al. 2018, AJ, 155, 107
Miller, G. H., Stolper, E. M., & Ahrens, T. J. 1991, JGRB, 96, 11849
Monteux, J., Andrault, D., & Samuel, H. 2016, E&PSL, 448, 140
Nguyen, T. G., Cowan, N. B., Banerjee, A., & Moores, J. E. 2020, MNRAS, 499, 4605
Nguyen, T. G., Cowan, N. B., Pierrehumbert, R. T., Lupu, R. E., & Moores, J. E. 2022, MNRAS, 513, 6125
Palme, H., & O'Neill, H. S. C. 2003, TrGeo, 2, 568
Pradhan, G. K., Fiquet, G., Siebert, J., et al. 2015, E&PSL, 431, 247
Quinn, S., Zieba, S., Cowan, N. B., et al. 2021, HST Proposal, 29, #16660
Schaefer, L., & Fegley, B. 2009, ApJL, 703, L113
Solomatov, V. S. 2000, in Origin of the Earth and Moon, ed. R. M. Canup et al. (Tucson, AZ: Univ. Arizona Press), 323
Tateno, S., Hirose, K., & Ohishi, Y. 2014, JGRB, 119, 4684
Tateno, S., Hirose, K., Sakata, S., et al. 2018, JGRB, 123, 5515
Tazieff, H. 1994, JVGR, 63, 3
Thomas, C. W., Liu, Q., Agee, C. B., Asimow, P. D., & Lange, R. A. 2012, JGR, 117, B10206
Usui, Y., & Tsuchiya, T. 2010, J. Earth Sci., 21, 801
Vinet, P., Ferrante, J., Rose, J., & Smith, J. 1987, JGRB, 92, 9319
Winn, J. N., Matthews, J. M., Dawson, R. I., et al. 2011, ApJL, 737, L18
Zhang, J., & Herzberg, C. 1994, JGRB, 99, 17729
Zieba, S., Zilinskas, M., Kreidberg, L., et al. 2022, A&A, 664, A79
Zilinskas, M., Miguel, Y., Lyu, Y., & Bax, M. 2021, MNRAS, 500, 2197
Zilinskas, M., Miguel, Y., Mollière, P., & Tsai, S.-M. 2020, MNRAS, 494, 1490